HAL
open science

Early molecular responses of mangrove oysters to nanoplastics using a microfluidic device to mimic environmental exposure

Adeline Arini, Zélie Venel, Hervé Tabuteau, Julien Gigault, Magalie Baudrimont

To cite this version:

Adeline Arini, Zélie Venel, Hervé Tabuteau, Julien Gigault, Magalie Baudrimont. Early molecular responses of mangrove oysters to nanoplastics using a microfluidic device to mimic environmental exposure. Journal of Hazardous Materials, 2022, 436, pp.129283. 10.1016/j.jhazmat.2022.129283 . insu-03690228

HAL Id: insu-03690228

https://insu.hal.science/insu-03690228v1

Submitted on 8 Jun 2022

HAL is a multi-disciplinary open access archive for the deposit and dissemination of scientific research documents, whether they are published or not. The documents may come from teaching and research institutions in France or abroad, or from public or private research centers.

L'archive ouverte pluridisciplinaire **HAL**, est destinée au dépôt et à la diffusion de documents scientifiques de niveau recherche, publiés ou non, émanant des établissements d'enseignement et de recherche français ou étrangers, des laboratoires publics ou privés.

Journal Pre-proof

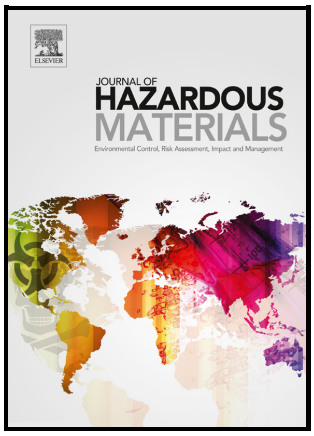

Early molecular responses of mangrove oysters to nanoplastics using a microfluidic device to mimic environmental exposure

Adeline Arini, Zélie Venel, Hervé Tabuteau, Julien Gigault, Magalie Baudrimont

PII: S0304-3894(22)01073-1

DOI: https://doi.org/10.1016/j.jhazmat.2022.129283

Reference: HAZMAT129283

To appear in: *Journal of Hazardous Materials*

Received date: 10 March 2022
Revised date: 25 May 2022
Accepted date: 31 May 2022

Please cite this article as: Adeline Arini, Zélie Venel, Hervé Tabuteau, Julien Gigault and Magalie Baudrimont, Early molecular responses of mangrove oysters to nanoplastics using a microfluidic device to mimic environmental exposure, *Journal of Hazardous Materials,* (2022) doi:https://doi.org/10.1016/j.jhazmat.2022.129283

This is a PDF file of an article that has undergone enhancements after acceptance, such as the addition of a cover page and metadata, and formatting for readability, but it is not yet the definitive version of record. This version will undergo additional copyediting, typesetting and review before it is published in its final form, but we are providing this version to give early visibility of the article. Please note that, during the production process, errors may be discovered which could affect the content, and all legal disclaimers that apply to the journal pertain.

© 2022 Published by Elsevier.

Journal Pre-proof

Early molecular responses of mangrove oysters to nanoplastics using a microfluidic device to mimic environmental exposure

Adeline Arini[1], Zélie Venel[1,2], Hervé Tabuteau[3], Julien Gigault[4], Magalie Baudrimont[1].*

[1] *University of Bordeaux, CNRS, UMR EPOC 5805, équipe Ecotoxicologie Aquatique, F-33120, Arcachon, France*

[2] *University of Rennes, CNRS, UMR Geosciences Rennes 6118, F-35000 Rennes, France*

[3] *University of Rennes, CNRS, IPR (Institut de Physique de Rennes), UMR 6251, F-35000 Rennes, France*

[4] *Université Laval, Département de Biologie, Pavillon Alexandre-Vachon, G1V 0A6, Québec, Canada*

*Corresponding author

Pr Magalie Baudrimont,
University of Bordeaux, CNRS, UMR EPOC 5805, équipe Ecotoxicologie aquatique
Station Marine d'Arcachon, Place du Dr Peyneau, 33120 Arcachon, France
Tel. +33(0)5 56 22 39 27
magalie.baudrimont@u-bordeaux.fr

Abstract

This study assessed the effects of nanoplastics (NPs) using for the very first time microfluidic devices (chip) mimicking transition waters. Three kinds of NPs were tested: crushed NPs from polystyrene pellets (NP-PS), or from Guadeloupe beaches (NP-G); and latex PS (PSL-COOH). The eluted fractions from the microfluidic device showed a low aggregation of NPs. They remained stable over time in the exposure media, with a stabilization of NPs of small sizes (< 500 nm). These chips were thus used for the toxicological assessment of NPs on swamp oysters, *Isognomon alatus*. Oysters were exposed for 7 days to the chip elution fraction of either NP-G, NP-PS or PSL-COOH (0.34 to 333 $\mu g.L^{-1}$). Gene transcription analyses showed that the tested NPs triggered responses on genes involved in endocytosis, mitochondrial metabolism disruption, oxidative stress, DNA repair, and detoxification. Highest responses were observed after NP-G exposure at low concentrations (1 $\mu g.L^{-1}$), as they are originated from the natural environment and accumulated contaminants, enhancing toxicological effects. As salinity influences aggregation and then the bioavailability of NPs, our results demonstrated the importance of using microfluidic devices for ecotoxicological studies on swamp or estuarine species.

Key words: Ecotoxicology, microfluidic device, swamp oysters, nanoplastics, gene transcription

Journal Pre-proof

INTRODUCTION

Within the size continuum of the plastics debris, nanoplastics (NPs) are the most worrying due to their nanometric size, shape, and surface charge which enables them to cross all biological barriers (cells, tissues) (Manfra et al., 2017, Gigault et al, 2021). Despite difficulties in detecting and quantifying these particles in complex organic matrices, a recent study has reported the presence of nanoscale plastics in seawater samples taken directly from the North Atlantic Gyre (Ter Halle et al., 2017). NPs' size is between 1 and 1000 nm, and they have a colloidal behavior in the environment (Gigault et al., 2018, Gigault et al, 2021). The adsorption of hydrophobic organic and inorganic compounds from the surrounding medium, such as metals, polycyclic aromatic hydrocarbons (PAHs) or polychlorinated biphenyls (PCBs), is facilitated by the hydrophobic properties and a high surface/volume ratio of NPs (Rochman et al., 2013b, 2013a; Velzeboer et al., 2014). Plastic are also made with additives such as plasticizers, that can represent up to 4% of their total weight (Andrady, 2011) or metals, such as oxo-fragmentable plastics (Anghelone et al, 2014). They can be released into the environment (Sajiki and Yonekubo, 2003; Teuten et al., 2009) or into the organs of aquatic organisms, inducing toxicity (Lithner et al., 2009).

The evaluation of the impact of NPs on organisms requires two mandatory considerations. It is crucial to consider the physico-chemical properties of the particles and their presence (concentrations) in the environment according to the natural features (ionic strength, pH, natural organic matter, etc.). To date, concerning the NPs' properties, most studies have used concentrations too high to be environmentally realistic (in the range of mg/L). There is hardly any data thus far for plastics at environmentally relevant concentrations and none are available for NPs. However, based on microplastic data, concentrations seem to range from 8 ng to 100 µg/L (Desforges et al, 2014; Goldstein et al, 2013). Moreover, while polystyrene was one of the least abundant plastics found in the North Atlantic gyre, compared to polyethylene, and polypropylene (Baudrimont et al, 2020, Ter Halle et al, 2017), most exposure studies were conducted using functionalized polystyrene latex nanosphere (PSL-COOH or PSL-NH_2) (Haegerbaeumer et al. 2019). Only a few studies have used nanoplastics released from plastics in the natural environment at relevant concentrations. A recent study used NPs made from polyethylene debris that had been collected in the North Atlantic gyre (1-1000 µg/L). The authors showed that these environmentally relevant NPs could impact algae and bivalves by inhibiting the cell growth of *Scenedesmus subspicatus* and incrementing the fecal and pseudo-fecal production of *Corbicula fluminea* (Baudrimont et al., 2020). Another study on mangrove oysters *Isognomon alatus* demonstrated that dietary exposure to nanoplastics (10-100 µg/L) produced from microplastics collected on Caribbean beaches could modulate genes involved in oxidative stress (up-regulation of the catalase gene) (Lebordais et al, 2021). Moreover, a recent study on *Isognomon alatus* demonstrated the synergic effect of arsenic (1 mg/L), when combined to NP exposures (7.5 to 15 µg/L) on response against oxidative stress (up-regulation of *cat*) and apoptosis (up-regulation of *bax* and *p53* genes) (Arini et al, 2022). However, even if these preliminary results demonstrated the need to work in environmental-like conditions, the

dynamics and the transport pathways of the nanoplastics from source to the organisms are not considered yet, especially towards environmentally relevant NPs.

Mangrove swamps are governed by extreme variations of abiotic and biotic features from the different estuarine systems. Indeed, two main sources of NPs can reach and remain captured in Guadeloupean mangroves : NPs brought by the North Atlantic oceanic gyre or NPs discarded from local terrestrial discharges (Ivar do Sul et al., 2014; Martin et al., 2019). These ecosystems are characterized by a stratification of freshwater and marine water separated by a salinity gradient due to the low water flow (Mohammed et al., 2014). To date, most studies have focused on the toxicity of plastic nanoparticles in fresh or marine waters but rarely in transitional waters. Bivalve can filter large amounts of suspended matters and water for nutritional and respiratory purposes as they are in permanent contact with the water column. This contributes to high bioaccumulation levels of pollutants (Arini et al., 2014; Baudrimont et al., 2005). *Isognomon* oysters are good models for studying the effects of sea pollutants since they are present worldwide in tropical seas, and especially in mangroves. Few studies investigated molecular biomarkers to characterize early responses triggered upon exposure to environmentally relevant micro- and nanoplastics, since more than 95% of studies are focusing on NP-PS to date (source Scopus 2021). A gene transcription-level change is a sensitive molecular biomarker that characterizes the toxicity of environmental pollutants towards cellular metabolism, oxidative stress, DNA damages, and apoptosis (Gonzalez et al., 2006). Recent studies in *Isognomon alatus* exposed to guadeloupean NPs have shown modulations in the expression of genes involved in responses including oxidative stress, at concentrations as low as 7.5 and 10 µg/L (Arini et al, 2022; Lebordais et al, 2021).

To date, the transportation pathways have not been considered in ecotoxicological studies. There is a real need to assess the environmental fate and behavior of nanoplastics in terms of stability, transport, and accumulation regarding the increase of ionic strength, the presence of natural organic matter, and their surface reactivity. Therefore, it is crucial to consider this dynamic, especially in the estuarine system, which is the main source of the inflow of the plastic debris from land to sea. Venel et al (2021) created a microfluidic chip to mimic the salinity gradients found in transition media, in order to be used for laboratory experiments. The authors demonstrated that the salinity gradient in the microfluidic device and the flow are conditioning the aggregation and transportation pathways of the NPs. The microfluidic device acts as a natural filter of nanoplastics based on their concentration, size, and shape properties (Venel et al, 2021).

In the present study, we used similar chip devices to investigate the relevant impacts of NPs within a salinity gradient on a tropical bivalve species: *Isognomon alatus*. We aimed to use this species as a model to explore the toxicity of NPs through a salinity gradient at environmental concentrations, in the range of µg/L. We hypothesized that the behavior, fate and toxicity of NPs could be modulated by the salinity gradient, compared to spiking studies, pouring NPs directly into salted water for ecotoxicological studies. For this aim, we used 1) NPs synthesized from crushed particles of plastics collected on the Guadeloupean marine coast (NP-G), 2) NPs synthesized from manufactured polystyrene pellets (NP-PS), and compare their impact to 3) carboxylated standard nanospheres (PSL-COOH). Finally, for the first time, we used

Journal Pre-proof

microfluidic devices to disperse plastic nanoparticles in a salinity gradient mimicking mangrove swamp as described in Venel et al (2021), before being poured into the exposure medium. This innovative approach will help increase understanding on the outcomes of exposures to NPs dispersed in a salinity gradient mimicking tropical areas such as mangroves, impacted by coastal as well as anthropogenic inputs of plastics.

MATERIALS AND METHODS

Oysters

Flat tree oyster *Isognomon alatus* (Gmelin, 1791) were collected in Guadeloupe by the University of the Antilles in the Grand Cul-de-Sac Marin (16°18'58.1460 "N 61°32'1.9379 "O), away from discharges and effluent wastewaters and considered as a clean area. Oysters were maintained three weeks in 50 L glass tanks (100 oysters per tank) filled with artificial seawater (ASW, Instant Ocean Salt, 30 g/L), at 26°C, oxygenated with aeration pumps, until used for experiments. A photoperiod of 12h light/12h dark was applied. Oysters were fed with two algal suspensions: *Isochrisis sp* and *Thalassiosira sp* (around 15 000 000 cell/ml, 20 mL per tank every two days). In case of oyster mortality, the organisms were immediately removed from tanks.

Nanoplastic preparation and characterization

Three different models of NPs were used and summarized in Table 1. We aimed to use crushed plastics of different shapes and at different sizes within a nanometric range, to mimic environmentally relevant NPs. The three models of NPs present a gradient in terms of environmental relevance for investigating their reliable and potential impact on organisms. 1) Crushed NPs were prepared from aged plastics collected on Guadeloupe beaches (16°21'06" N 61°23'09" W) in 2016 according to El Hadri and al. (2020), to mimic the shape and size and composition heterogeneity of NPs that were observed in the real environment. Plastic pieces collected on Guadeloupe beaches were used to obtain a mix composed of 90% polyethylene and polypropylene nanoparticles (NP-G). Previous studies showed that the crushed NP solution was highly polydisperse, and that NPs presented different shapes and negatively charged surfaces. It was therefore very close to environmental nanoplastics in terms of chemical nature and morphology (El Hadri et al, 2020). 2) Virgin polystyrene pellets were used to obtain polystyrene nanoparticles (NP-PS), commonly used in the literature. 3) Finally, to better illustrate the importance of the environmental relevance of the NP-G used in this study, we compared them with polystyrene standard nanospheres with carboxylate functions (PSL-COOH) conferring negative charge on their surface (Polyscience) like NP-G. The PSL-COOH is 200 nm in diameter and has an unknown surfactant composition. All nanoparticles were dispersed in deionized water (18 MΩ cm^{-1}, Millipore water purification system, Merck, Darmstadt, Germany). Table 1 summarizes nanoparticles characteristics and the exposure conditions of oysters. Hydrodynamic diameters of NPs (Z-average) were assessed by dynamic light scattering (DLS) using a Vasco-Flex model particle size analyzer (Cordouan Technologies, Pessac, France). The organic carbon concentration of NP samples was determined using a total organic

carbon instrument (Shimadzu, Kyoto, Japan) and related to the known percentages of polymers (mainly PE and PP) present in the NP sample. The surface charge of NPs was determined using a Wallis zetameter (Cordouan Technologies). The particle concentrations were measured by Laser induced breakdown detection (LIBD, Cordouan Technologies) which gives the number of particles/mL. The NP-PS dispersion was composed of two populations of 250±50 and 390±20 nm (Figure SI.2A in SI). NP-G dispersion constituted two populations of 52±20 nm and 115±20 nm with some particles around 620±70 nm (Figure SI.2B in SI). Exposure of oysters was performed with nanoparticle concentration in the µg L^{-1} range. Since the average diameter of nanoparticles is relatively close to each other, we consider that mass concentration and particulate concentrations are equivalent and comparable between each nanoparticles type (for a 1 µg L^{-1} mass concentration, particular concentrations vary from 5.6 10^4 to 1.78 10^5 particle mL^{-1}).

Table 1: Plastic nanoparticles characteristics and exposure concentrations

	Stock dispersion concentration (ppm)	Z-average (nm)/PDI (pH7)	Zeta potential (mV)	Oyster exposure concentration (µg L^{-1})				
				Control	C1	C2	C3	C4
NP-PS	50	319/0.20	-44 ± 2	0	4	37	222	333
NP-G	20	220/0.21	-30 ± 2	0	1	15	44	133
PSL-COOH	200	217/0.048	-38.6 ± 2	0	0.34	1		

Experimental design

Each experimental unit was filled with 1 L of artificial seawater (ASW, Instant Ocean Salt, 30g L^{-1}) maintained at 26°C and oxygenated with an aeration pump. Four oysters were introduced in each glass tank 24h before the start of the experiment. Oysters were fed 2h before the start of the experiment, with 10 mL of *Isochrisis sp* algae (15 000 000 cell mL^{-1}). Temperature, salinity, pH, and water levels were checked daily and adjusted when necessary. The microfluidic device described by Venel et al. (2021) was used to study the fate of NPs through a salinity gradient. In this study, the two outlets of the microfluidic device were placed directly in the exposure tank, as illustrated in Figure 1. Indeed, this study aims to mimic the transportation of NPs from freshwater to marine water. At Day 0, the experimental units were gradually exposed through a microfluidic device at 2 to 6 mL of NPs depending on the initial concentration to reach final concentrations summarized in Table 1. The stability of NPs models was investigated before oyster exposure (see supplemental information, Fig SI3, and SI4). Results showed that the NP-G and NP-PS solutions had good size stability over 24 h after passing through the microfluidic device. Oysters were dissected after 7 days of exposure to NPs. Gills and visceral mass were collected from two individuals of the same experimental unit and pooled to obtain enough tissue

Journal Pre-proof

mass for analysis. Samples were stored at -80°C in 500 µL of RNA Later until being processed for gene expression analysis.

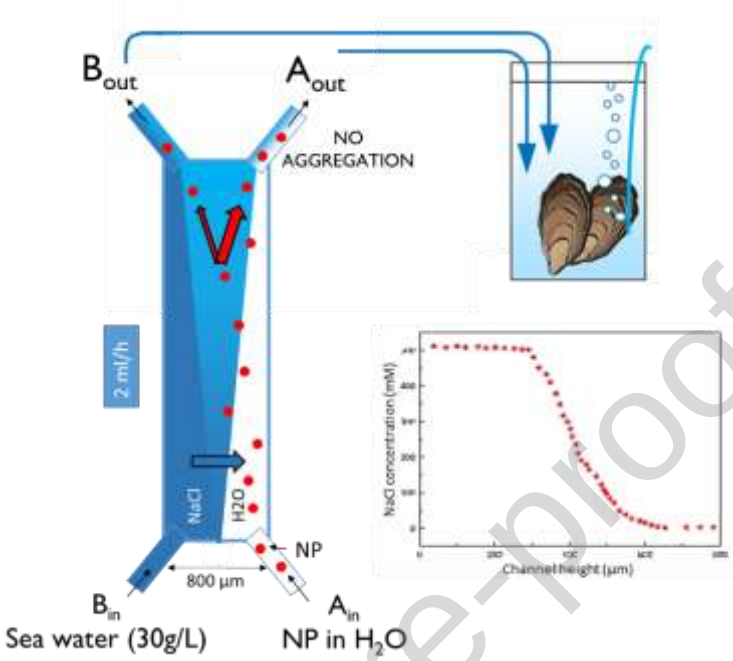

Figure 1: Experimental design: dispersion of NPs through a salinity gradient in the microfluidic device. The two outlets of the microfluidic device plunged into the exposure unit.

Design of primers

Primers were obtained as described in Arini et al (2022). Briefly, *Isognomon alatus'* transcriptom was obtained after assembling the sequences from Lemer et al. (2019) with the Trinity tool provided by the Galaxy server (https://usegalaxy.org/). Target genes were involved in endocytosis, detoxication, respiratory chain, oxidative stress, DNA repair, and apoptosis (Table 2).

Table 2: Genes names, functions, and nucleotide sequences. [a]Forward primer, [b] Reverse primer.

Gene	Name	Function	Sequence 5'-3'
β actin	Beta Actine	Housekeeping gene	AACGAGCGATTCAGATGTCC[a]
			CGATTCCTGGGtACATGGTT[b]
rpl7	Ribosomal protein L7	Housekeeping gene	CCCAGGAAGGTCATGCAGTT[a]
			TCCCAGAGCCTTCTCGATGA[b]
cltc	Clathrin heavy chain	Endocytosis	AGACTCAGGACCCAGAGGAC[a]
			ATCACACGGGTTCTATCGGC[b]
cav	Caveolin	Endocytosis	CGTCGAGATCCAGACCTGTT[a]

Journal Pre-proof

			ACAGCATTGACTGCGTATGG[b]
mdr	ATP Binding Cassette Subfamily	Detoxication	GCATGTTGCAAGCCTGTCAA[a]
			CAGTCAACTCAAGCAACCGC[b]
cox1	Cytochrome C oxidase	Mitochondrial metabolism	GTTGCCTTGGTCGCTAGACT[a]
			GAGCGTCTTGGGCTTAGTCA[b]
12s	Mitochondrial 12s rRNA	Mitochondrial metabolism	TCAGGTGTTACACAGCCGTC[a]
			GCAGGCGTTTTAATCCCGTC[b]
cat	Catalase	Oxidative stress	CGAGGCTAGCCCAGACAAAA[a]
			TTGGGGAAATAGTTGGGGGC[b]
sod1	Superoxide dismutase 1	Oxidative stress	AGACTGCGTCACATGCTTCA[a]
			GCGTCATGTAGGGGATCTGG[b]
gadd45	Growth Arrest and DNA Damage	DNA repair	TTGGCTTGACAAAAGTGCCG[a]
			CTGACAACCTGCATCTCGGT[b]
p53	Tumor protein p53	DNA repair, apoptosis	CGATGATCGGGTTCAGCAGA[a]
			GAGCTCTCTCAACACAGCCA[b]
gapdh	Glyceraldehyde-3-phosphate dehydrogenase	Apoptosis, DNA repair, and oxidative stress	CACGGCAACACAGAAGGTTG[a]
			CCCTTCTGAAGTCGGCAAGT[b]
bax	BCL2 Associated X-protein	Apoptosis	AACTGGGGCAGAGTTGGATG[a]
			AATTGCTTCCCAGCCTCCTC[b]

We used two housekeeping genes (*β actin* and *rpl7*) as reference. The geometric mean of these two reference genes was used to normalize target gene expression. There was no significant difference in their expression among the different treatments (data not shown).

Gene transcription analyses

Two organs of the oysters were assayed for the differential gene expression : gills (G) and visceral mass (VM). The total mRNA extraction was performed with the SV Total RNA Isolation System (Promega), according to the manufacturer's instructions. total. It was followed by a reverse transcription (RT), using the GoScript Reverse Transcription System (Promega) (for details, see Arini et al., 2022). cDNA was synthesized from RNA samples in an Eppendorf Mastercycler and kept at -20°C until their use for real-time qPCR amplification.

Real-time PCR reactions were performed in a LightCycler 480 (Roche) to quantify cDNA amplification using a kit GoTaq® qPCR Master Mix (Promega) as described in Arini et al (2022). The specificity of each gene amplificon was checked with the dissociation curve of PCR products after gradual heating from 60 to 95°C.

Two reference genes (*β-actin* and *rpl7*) were used to normalize the relative quantification of each gene expression (according to the GeNorm method). The differential gene expression was calculated using the $2^{-\Delta Ct}$ method described by Livak and Schmittgen (2001). Induction factors

Journal Pre-proof

of gene expression were calculated between exposed and control samples according to the following equation:

$$IF = \frac{2^{-\Delta Ct\ exposed}}{2^{-\Delta Ct\ control}}$$

Metal analysis

Metal analyses were performed using a Quadrupole ICP-MS (Agilent Technologies 7700x). We carried out metal analyses in plastic samples due to their high adsorption capacities, and due to their intrinsic composition that can be made of metals (for colour or fragmentable properties for instance) (Anghelone et al, 2014). The concentrations were determined using a conventional external calibration procedure with a multi-elemental solution acidified to 2% in HNO_3. A Rhodium solution was used as an internal standard to correct the instrumental drift and potential matrix effects. For NP-G, total digestion of the solutions was performed using nitric acid (14N HNO_3) at 100°C for 24h. After complete evaporation, the residue was solubilized in 0.37N HNO_3. We used a previous strategy for leaching experiments of metals adsorbed to the microplastics' surface (Catrouillet et al, 2021). This method consists of adding HNO_3 (2% wt) to plastic debris, stirring for 24h, and then filtering the microplastics from the HNO_3 solution.

Statistics

Significant differences between treatments were revealed using statistical tests. Normality and homoscedasticity of distribution were checked using Shapiro Wilk and Levene test. Data were converted to a normal distribution when necessary using box-cox transformation. If normality and homoscedasticity criteria were respected, ANOVA or T-test between control and contaminated conditions were applied, followed by Tuckey HSD post hoc. Otherwise, the non-parametric Kruskal-Wallis test was performed with post hoc U Mann-Whitney (Statistica 8). A probability of $p < 0.05$ was considered significant for all statistical tests.

RESULTS

Size evolution of the nanoplastic models in the different microfluidic outlets

Figure 2 illustrates the size evolution of the nanoplastics (11 mg/L) in the microfluidic outlets. The eluted nanoparticles in both outlets at constant concentrations are stable against ionic strength, especially those encountered in the marine environment. Based on this observation, both outlets are connected to the exposure medium in the exposition set-up. The final population is governed as a mixture of populations from the two outlets (A and B).

Carboxylated polystyrene sphere nanoparticles (PSL-COOH) present no size evolution (i.e., 200nm) from the two outlets. This result confirms the significant stability of the carboxylated spherical nanoparticles in aqueous media against the ionic strength' increase. The deprotonated carboxylate function at the particle's surface induced enough repulsion between particles to promote stability, which is unusual in environmental media.

Journal Pre-proof

For the NP-PS and NP-G, the transportation through the salinity gradient in the microfluidic device induces (i) a loss of particles that are aggregating and trapped in the device (ii) a fractionation of the eluted particle according to their size. The eluted fractions remain stable over time in the final exposure media, even at high concentrations (SI4). For both nanoplastics models, NP-G and NP-PS, two central populations are considered: a small size around 400-500 nm and a second one from 0.7 up to 2µm. The difference in these sizes is due to the the initial size is significantly higher for the NP-G (SI2, around 650 nm).

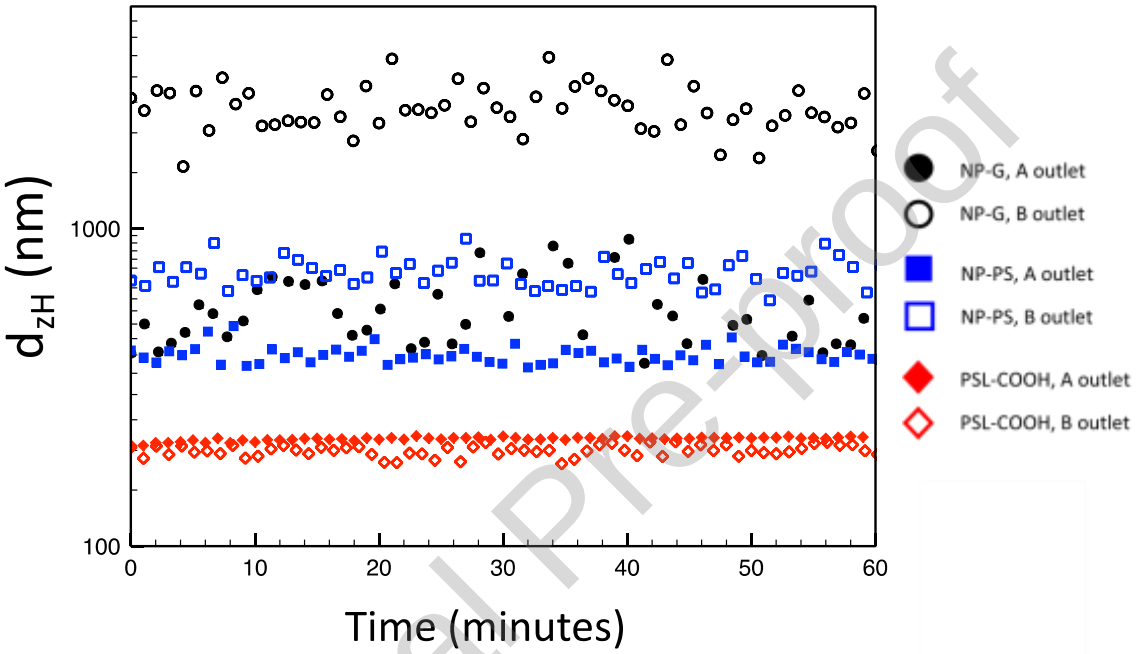

Figure 2: Size evolution of the NP models in the different microfluidic outlets (A and B).

Trace metal quantification

Total and adsorbed trace metals concentrations have been measured for NP-G (Figure 3). Results of absorbed metals showed a high concentration of aluminum, iron, and zinc adsorbed onto plastic pieces from Guadeloupe beaches (between 200 and 6000 µg kg^{-1}) and a low concentration of arsenic, lead, and cadmium (mean of 32 and 13.9 and 13.9 µg kg^{-1} respectively). Total trace metal concentrations were higher and showed a high proportion of aluminum, iron, lead, and zinc (60-200 mg kg^{-1}).

Journal Pre-proof

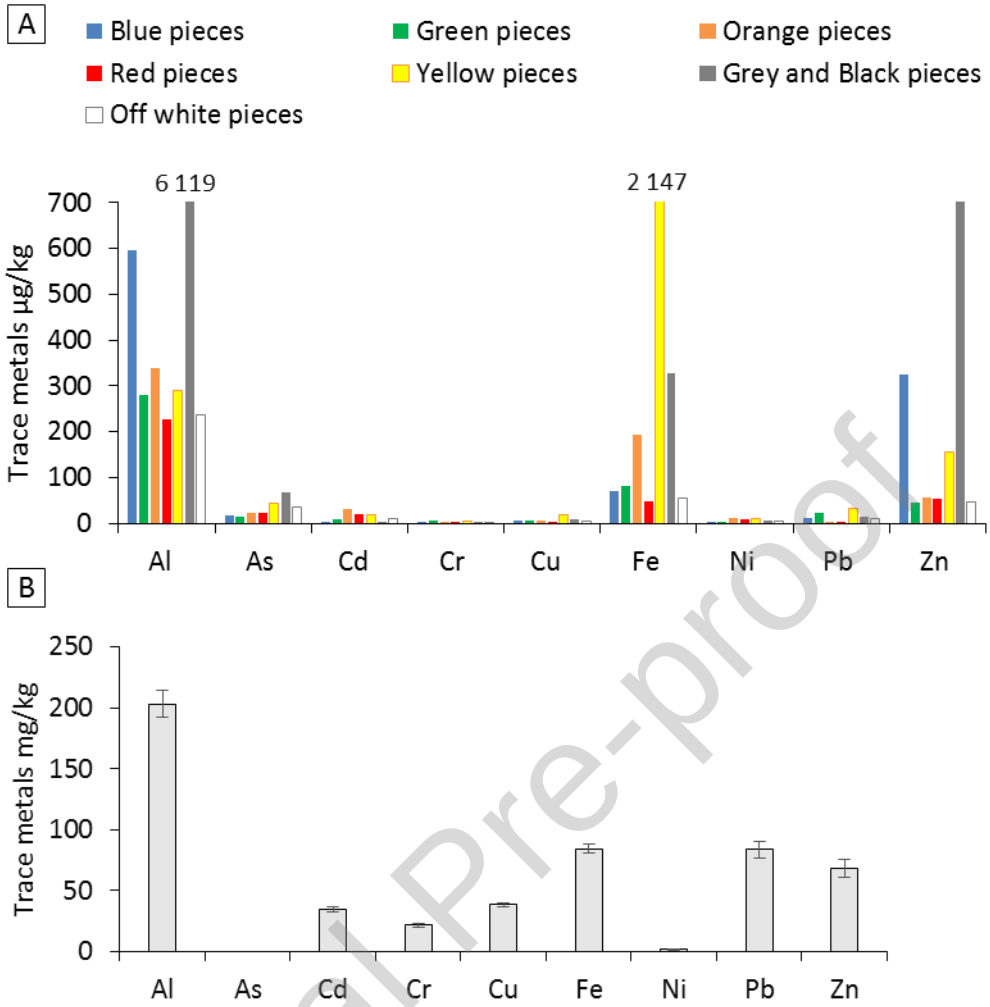

Figure 3: Trace metals quantification in NP-G. A: trace metals adsorbed on the surface of plastic pieces; B: total trace metals obtained after total acid digestion of NP-G powder.

Gene transcription results

Overall, the three different kinds of NPs used to expose oysters led to significant changes in gene expression in gills and visceral mass of oysters after the exposure to NP-G (50 and 61% respectively), NP-PS (59 and 52%, respectively), and PSL-COOH (45 and 55%, respectively) (Table 4).

NP-G

NP-G showed a reverse dose-response relationship with exposure concentrations. Compared to others, more genes were significantly modulated at the lowest concentration C1 (1 µg L^{-1}, 64% and 73% in gills and visceral mass, respectively).

In gills, the caveolin-dependent endocytosis was implemented at low NP concentrations (6.57 and 1.9 fold-changes for 1 and 15 µg/L, respectively) and tended to decrease in favor of clathrin-dependent endocytosis at high concentrations (4.09 to 7.53 fold-changes for 15 to 133 µg/L).

Journal Pre-proof

The NP-G exposure significantly impacted mitochondrial metabolism. There was a strong induction of the *mdr* detoxication gene at the lowest NP-G concentration (11.48 fold-change) observed for higher NP concentrations. The *12s* gene was induced in oysters exposed to each concentration tested (2.11 to 7.30 fold-changes), and *cox1* was only induced after the exposure to C3 (44 µg/L). The exposure to NP-G did not lead to DNA repair, but the pre-apoptotic gene *p53* was induced in oysters exposed to C1 (1 µg/L) (4.41 fold-change). An apoptotic response was observed through the over-expression of *bax*, in gills of oysters exposed to C2 (15 µg/L) and C4 (133 µg/L) (2.38 and 3.70 fold-changes, respectively).

In visceral mass, the endocytosis of NP-G occurred only via the caveolin pathway, with strong gene inductions for each concentration tested (up to 85.15 in the C1 condition). It was concomitant with strong inductions of the detoxication gene *mdr*, for each NP-G treatment (up to 40.70 in C1 the condition). Significantly few effects were observed on the mitochondrial metabolism, with an induction of the *12s* gene only for the highest NP-G concentration (3.13 fold-change). In contrast, the *cox1* gene was repressed in the C1 and C4 conditions. Opposite patterns were observed for the two genes involved in oxidative stress. All concentrations tested led to a repression of the *cat* gene (0.03 to 0.39 fold-changes), whereas they led to an induction of the *sod1* gene (2.92 to 4.04 fold-changes). The response in DNA repair was weak (1.6 fold-change for *gadd45* in the C3 condition). In gills, *p53* was only induced in the C1 condition (3.63 fold-change). The apoptotic response was mainly implemented by the up-regulation of the *bax* gene (2.85 to 3.19 fold-changes for C2 to C4 conditions, respectively). In comparison, the *gapdh* gene was down-regulated (0.08 to 0.31 fold-changes).

NP-PS

Like NP-G, the NP-PS showed a reverse dose-response relationship with high genes responses at the lowest concentration C1 (4 µg L^{-1}). Indeed, 82% of genes were significantly modulated in both gills and visceral mass in the C1 condition, whereas only 55 and 27% were modulated in the C4 (333 µg L^{-1}) condition, respectively. NP-PS caused more damages in the visceral mass at low concentrations, whereas effects were more pronounced in gills at high concentrations. Since NP-PS were made from virgin polystyrene pellets, no chemical adsorbed onto their surface nor toxic pigments could be released and cause adverse effects.

In gills, the NP-PS endocytosis mainly occurred via the clathrin pathway. In an inverse dose-response manner, the gene was strongly up-regulated for each concentration tested (3.74 to 109 fold-changes). The caveolin endocytosis was also implemented to a lesser extent (1.75 to 2.53 fold-changes for C1 to C3 conditions). The *mdr* gene was induced in C1, C2 (37 µg L^{-1}), and C3 (111 µg L^{-1}) conditions (2.89, 3.09, 3.57 fold-changes, respectively). The genes involved in the mitochondrial metabolism were strongly modulated for each concentration tested, with induction factors higher than for the NP-G exposures (2.81 to 19.78 fold-changes for *12s* and 4.33 to 7.58 for *cox1*). It is worth noticing that the fold-changes of *12s* and *cox1* followed opposite patterns. Strong inductions of *cat* were observed in gills of oysters exposed to C1 and C4 (11.73 and 19.01 fold-changes, respectively), whereas *sod1* was repressed at the same concentrations tested (0.12 and 0.43, respectively). Significant induction of the *gadd45* gene revealed the implementation of DNA repair for the C1 to C3 conditions (3.21 to 4.79 fold-

changes). However, a weak apoptotic response was observed with *p53* induced only in the C1 condition (2.94 fold-change) and *bax* only in the C4 condition (2.48 fold-change).

Due to analytical issues, no data was available for the C2 condition in visceral mass. However, as for NP-G exposures, the results showed strong induction of the caveolin gene (81.05 and 7.35 fold-changes for C1 and C3, respectively), concomitant with high inductions of the detoxication gene *mdr* (34.34, 4.75, 1.74 fold-changes for the C1, C3 and C4 conditions, respectively), both gene following a reverse dose-response relationship. The genes involved in the mitochondrial metabolism were up-regulated only in the highest concentrations tested (2.59 and 2.07 fold-changes in the C3 and C4 conditions, respectively for 12s; 1.72 fold-change in C4 for *cox1*). A response against the oxidative stress was observed through the up-regulation of *sod1* (11.31 and 1.56 fold-changes in C1 and C3, respectively), whereas *cat* was down-regulated in the C1 condition (0.07 fold-change). The DNA repair was induced in oysters exposed to the C3 condition (1.96 fold-change). Still, as for gills, a weak apoptotic response was observed with *p53* and *bax* only induced in the C1 condition (9.48 and 2.66 fold-changes, respectively) while the expression of *gapdh* was repressed (0.21).

PSL-COOH

PSL-COOH was the more stable against the increase of the ionic strength in the solution and exhibited the smallest sizes of nanoparticles in the solution. Unlike other NPs tested in this study, PSL-COOH induced gene modulations in a dose-response manner. In the C1 (0.34 µg L^{-1}) condition, 27 and 54% of genes were modulated, whereas 45 (despite the lack of data) and 54 % were modulated in the C2 (1 µg L^{-1}) condition, in gills and visceral mass, respectively

In gills, the endocytosis patterns seem to be governed by the caveolin gene (3.6 fold-change in the C2 condition (1µg/L)) and are followed by a detoxication (5.6 fold-change in the C2 condition). Like the other NP exposures, the genes involved in the mitochondrial metabolism were up-regulated (2 fold-change for *12s* in the C2 condition; 2.49 and 3.3 fold-changes in the C1 and C2 conditions for *cox1*). Catalase was induced in the C1 condition (4.36 fold-change), but no modulation of the *sod1* gene could be observed (note that some data are missing). Even with the lack of data in the C2 condition, results showed that the exposure to PSL-COOH could lead to the implementation of DNA repair and apoptosis (6.3 fold-changes for *gadd45* in C; 2.17 fold-change for *gapdh* in C1).

In the visceral mass, unlike for others NPs tested, PSL-COOH led to the implementation of endocytosis through the clathrin pathway (3.83 and 2.62 fold-changes). No detoxication was observed via the *mdr* gene. However, strong inductions of the genes involved in the mitochondrial metabolism occurred for both concentrations tested (up to 7.74 for *12s* and 8.35 for *cox1* in C2 and C1, respectively). Interestingly, no response against oxidative stress was observed after PSL-COOH exposure, as the *cat* and *sod1* genes were down-regulated. DNA repair was implemented in oysters exposed to the C1 concentration (2.19 fold-change of gadd45), but no apoptotic response could be observed through the *p53* and *bax* genes.

Journal Pre-proof

DISCUSSION

Microfluidic

Generally, high ionic force tends to aggregate nanoparticles if the collision efficiency between particles is sufficient, as shown in Figures SI3 and SI4 and elsewhere (Chen and Elimelech, 2006; Venel et al., 2021). Transportation of nanoparticles through a salinity gradient in the microfluidic chip led to natural aggregation with a fraction of larger size deposited and another fraction remaining stable and transported to high ionic strength'. Using the same microfluidic approach, we recently demonstrated that one fraction of the NP-PS aggregate to form large particles, which either float or sediment. This fraction becomes trapped in the microfluidic device (Gigault et al, 2018).

We used a Laser induced breakdown method (LIBD) to measure the remaining fraction of particles and estimated that only 10% of the initial NP concentration crosses the B outlet and reaches the exposure medium. This fraction transported through the salinity gradient without depositing was stable due to the dilution. Indeed, this behavior is explained by the collision rate and the diffusiophoresis phenomena occurring within the salinity gradient in the microfluidic device (Venel et al 2021). As particles are too far from each other, the collision probability is lower (Venel et al., 2021). If this behavior in the salinity gradient is not taken into account in the exposure experiment, the toxicity of nanoplastics would remain largely biased and underestimated.

Gene transcription changes

All the gene expression results in gills and oysters' visceral mass are synthesized for low doses of exposure in Figure 4.

By comparing the effects at gene level for similar high concentrations of NP-G and NP-PS (C4 : 133 µg/L; and C3 : 111 µg/L, respectively), we can attest that NP-G triggered more effects than NP-PS, with 59 and 50% of genes modulated, respectively. At low concentrations, we observed the opposite pattern with more genes modulated after NP-PS exposures (1 to 44 µg L^{-1}) compared to NP-G. This suggests that oysters were exposed to concentrations around ten times lower than the nominal ones. These results can then be compared to a recent study on *Isognomon alatus*, spiking NP-G and NP-PS solutions through the direct route and without using microfluidic devices. The authors showed that NP-G generated more significant changes in gene expressions than NP-PS after a one-week exposure at concentrations between 7.5 and 15 µg/L (Arini et al, 2022). The authors suggest that the sorption of xenobiotics onto surfaces of NPs coming from natural sources may enhance their biological impacts on oysters. Indeed, NP-G is originated from naturally aged plastics in the environment. NPs have been shown to carry pollutants onto their surface like persistent organic pollutants or trace metals released inside the cells (Cole et al., 2011; Koelmans et al., 2016). Analyses of trace metals showed a strong absorption of aluminum, iron, and zinc onto plastic pieces from Guadeloupe beaches and, to a lesser extent, the presence of arsenic, lead, and cadmium. Those trace metals are toxic, as demonstrated elsewhere (Barjhoux et al., 2012; Baudrimont et al., 2019; Freitas et al., 2018;

Journal Pre-proof

Gonzalez et al., 2006; Koelmans et al., 2015; Lu et al., 2018; Moreira et al., 2018) and could lead to additional toxic effects in oysters exposed to NP-G.

In comparison, a study on dietary-exposed swamp oysters (fed one week with algae exposed to 10 or 100 µg/L) showed that NP-PS could trigger more effects at the gene level than NP-G (Lebordais et al, 2021). It seems that the NP composition and behavior can influence NPs' toxicity on aquatic organisms. The exposure route appears to be a crucial criterion to be taken into account for their study in ecotoxicology.

Interestingly, the present study showed that the effects of NPs on gene expression were not dose-dependent, with lower effects at the highest concentrations tested for NP-G and NP-PS. PSL-COOH induced the lowest impact on genes compared to other NP types. The shape of nanoparticles could explain the higher impact of NP-G and NP-PS. Indeed, they have irregular shapes, nearly fractal (see Figure SI1). These results also follow the spiking study of Arini et al. (2022). These two studies are the first evidence supporting behavioral changes when oysters are exposed to high NP concentrations. Indeed, a few studies have so far reported that mussels exposed to microplastics could decrease their filtration rates and reject plastic particles into their pseudofeces (Wegnet al. al, 2012; Woods et al., 2018). In Arini et al. (2022), the authors hypothesized that the valve closure observed in oysters exposed to high concentrations of NPs could result from the NP aggregation, trapped and rejected in mucus through pseudofeces. Mucus secretion has been shown to sequestrate particles outside tissues, thus protecting cells from particle penetration (Handy et al., 2008). The present study notes that high mucus secretion leading to deposit on tank walls was observed in experimental units with the highest concentrations of NP-G and NP-PS. This cannot be related to aggregation phenomena since microfluidic devices tend to avoid aggregation of NPs. This suggests that other phenomena may also influence the ventilatory activity of oysters exposed to NPs. Due to the high salinity and the probable presence of organic matter coming from oysters, NPs could also have formed heteroaggregates that may decrease bioavailability of NPs.

Results showed that both caveolin and clathrin-dependent endocytosis pathways were implemented after NP-G, NP-PS, and PSL-COOH exposures. The privileged endocytosis process was clathrin-dependent in gills, which are the first barrier to contact the surrounding medium. Indeed, some authors suggested that the mechanisms of the internalization of negatively charged NPs in aquatic organisms occur via clathrin pathways (Kögel et al., 2020). These results are exciting compared to two previous studies on *Isognomon alatus*, exposed to similar NP-G and NP-PS solutions, but via different entry routes, namely waterborn and dietborn (Arini et al., 2022; Lebordais et al., 2021). The authors did not report any modulation of caveolin or chlathrin in oysters after NP exposures in both aforementioned studies. They hypothesized that endocytosis was mainly implemented for small particles and that NP sizes may have been too large to be taken by those mechanisms. The differences between their results and the present study lie in microfluidic devices. This study showed that microfluidic devices efficiently avoid most NP aggregation and truly test NP toxicity at a nanometric scale. The smallest size fractions of NPs plunged into the medium at the device outlets were comprised between 200 and 500 nm corresponding to the maximum nanoparticle sizes that endocytosis could carry by caveolin process (Mo et Lim, 2004; Rejman et al., 2004). Since PSL-COOH has

Journal Pre-proof

a size of 200 nm and is very stable in high salinity, they could also be taken by clathrin-dependent endocytosis, which can internalize nanoparticles up to 200 nm (Rejman et al. 2004).

Concerning MXR transporters, the exposure to the three types of NPs led to increased expression of the *mdr* gene, involved in detoxication. Detoxication was very active in the visceral mass as this organ is known for its storage, metabolic and detoxication functions (Marigomez et al., 2002). However, no such results were found in the literature concerning similar negatively charged NPs. Arini et al. (2022) and Lebordais et al. (2021) showed that oysters' waterborne and dietborne exposures to NPs did not increase the *mdr* gene expression. This indicates that detoxication through the *mdr* gene can, at least in part, be tuned by particle size. Microfluidic devices may be responsible for the differences observed between their results and the present study, resulting in smaller NPs.

There are scarce data available in the literature about the potential of NPs to generate oxidative stress. All three NPs tested led to effects at the mitochondrial level with an increase of *12s* and *cox1* expressions (except for NP-G in visceral mass). A strong up-regulation was also demonstrated in Arini et al (2022) study on *Isognomon alatus*, exposed through direct route to NP-G and NP-PS, but not after dietborne exposures (Lebordais et al 2021). It suggests that even with implementing the detoxication mechanism, through the MDR pathway, the exposure to NPs through microfluidic devices generated mitochondrial stress, resulting in the production of reactive oxygen species in cells. Indeed, oxidative stress was observed in each condition tested through the up-regulation of *cat* and *sod1* genes. We expected higher effects in oysters exposed to NP- G, which originated from naturally aged plastics in the environment, and lower effects in oysters exposed to NP-PS and PSL-COOH, supposedly not containing surfactants. However, no clear trend could be observed on oxidative stress. Several studies have shown that additives are present in commercial latex, like surfactants (Hrenovic and Ivankovic, 2007; Jahan et al., 2008; Rosety et al., 2001) and biocides (Pikuda et al., 2019) and can disturb cell functions. Jeong et al. (2016) showed that 50 and 500 nm PSL at 10 µg mL^{-1} induced an increase of ROS level compared to the control in rotifer after 24h of exposure. 50 nm PSL also increased SOD, GST (Glutathione S-transferase), GR (Glutathione reductase), and GPx (Glutathione peroxidase) antioxidant proteins activity, whereas 500 nm PSL increase only GR and GST activities. Additives like plasticizers are also present in commercial NP-PS (Lithner et al., 2011, 2009; Teuten et al., 2009; Yin et al., 2018). Compared with a spiking study, with NP-G and NP-PS (Arini et al, 2022), we note clear differences as *cat* and *sod1* were repressed, whereas they were strongly induced in the present study. Again, this reiterates the importance of considering the exposure route and NPs behavior along salinity gradients.

The DNA repair and pre-apoptotic responses were implemented in oysters exposed to NP-PS and PSL-COOH, and a lesser extent to the ones exposed to NP-G. As a result, the apoptotic response was more robust through bax expression in the NP-G conditions than NP-PS and PSL-COOH. These results follow the previous spiking study where the authors showed that the exposure of oysters to NP-G could lead to an up-regulation of *p53* and *bax* genes (Arini et al., 2022).

Journal Pre-proof

By comparing microfluidic and spiking approaches, we can attest that the microfluidic study's effects on gene expression are robust. This probably relies on a better NP internalization through endocytosis pathways that the detoxication mechanisms (MDR) seem unable to counteract entirely. It is followed by oxidative stress that can lead to stronger adverse effects, such as apoptosis, compared to traditional studies not using such microfluidic devices. These results underline the lack of data on relevant environmental conditions, especially concerning transition waters such as mangroves, where salinity gradient may vary.

Table 4: Differential gene expression observed in gills and visceral mass of oysters after direct contamination with NPs through MD. Only statistically significant results are reported. Results are given as induction (>1) or repression (<1) factors as compared to control oysters. -: identical to control levels. NA: not available.

Organ and function	gene	NP-G				NP-PS				PSL-COOH	
		C1	C2	C3	C4	C1	C2	C3	C4	C1	C2
		1	15	44	133	4	37	111	333	0,34	1
		µg L^{-1}									
Gills											
Endocytosis	*cav*	6.57	1.9	-	0.21	1.75	2.38	2.53	-	-	3.6
	cltc	-	4.09	7.12	7.53	109	104	50	3.74	-	NA
Detoxication process	*mdr*	11.48	-	-	-	2.89	3.09	3.57	-	-	5.6
Mitochondrial metabolism	*12s*	7.30	2.11	4.37	6.24	19.78	11.68	12.68	2.81	-	2.0
	cox1	-	-	3.44	-	7.58	6.73	5.90	4.33	2.49	3.3
Oxidative stress	*cat*	0.30	-	3.94	2.98	11.73	-	-	19.01	4.36	NA
	sod1	2.19	1.85	-	-	0.12	-	-	0.43	-	NA
DNA repair	*gadd45*	-	0.55	-	-	3.21	4.89	4.79	-	-	6.3
DNA repair or apoptosis	*p53*	4.41	-	-	-	2.94	-	-	-	-	NA
Apoptosis	*bax*	-	2.38	-	3.70	-	-	-	2.48	-	NA
Apoptosis	*gapdh*	0.17	-	-	-	-	-	-	-	2.17	NA
Visceral mass											
Endocytosis	*cav*	85.15	15.06	5.39	32.44	81.05	NA	7.35	-	-	-
	cltc	0.35	-		-	0.15	NA	-	-	3.83	2.62
Detoxification process	*mdr*	40.70	6.44	3.44	4.96	34.34	NA	4.75	1.74	0.42	-
Mitochondrial metabolism	*12s*	-	-	-	3.13	-	NA	2.59	2.07	6.37	7.74
	cox1	0.20	-	-	0.39	-	NA	-	1.72	8.35	6.75
Oxidative stress	*cat*	0.09	0.19	0.03	0.39	0.07	NA	-	-	-	0.05
	sod1	3.66	2.99	2.92	4.04	11.31	NA	1.56	-	0.29	0.13
DNA repair	*gadd45*	-	-	1.6	-	0.42	NA	1.96	-	2.19	-
DNA repair or apoptosis	*p53*	3.63	-	-	-	9.48	NA	-	-	-	-
Apoptosis	*bax*	-	2.85	2.90	3.19	2.66	NA	-	-	-	0.51
	gapdh	0.08	0.31	-	0.23	0.21	NA	-	-	-	-

Journal Pre-proof

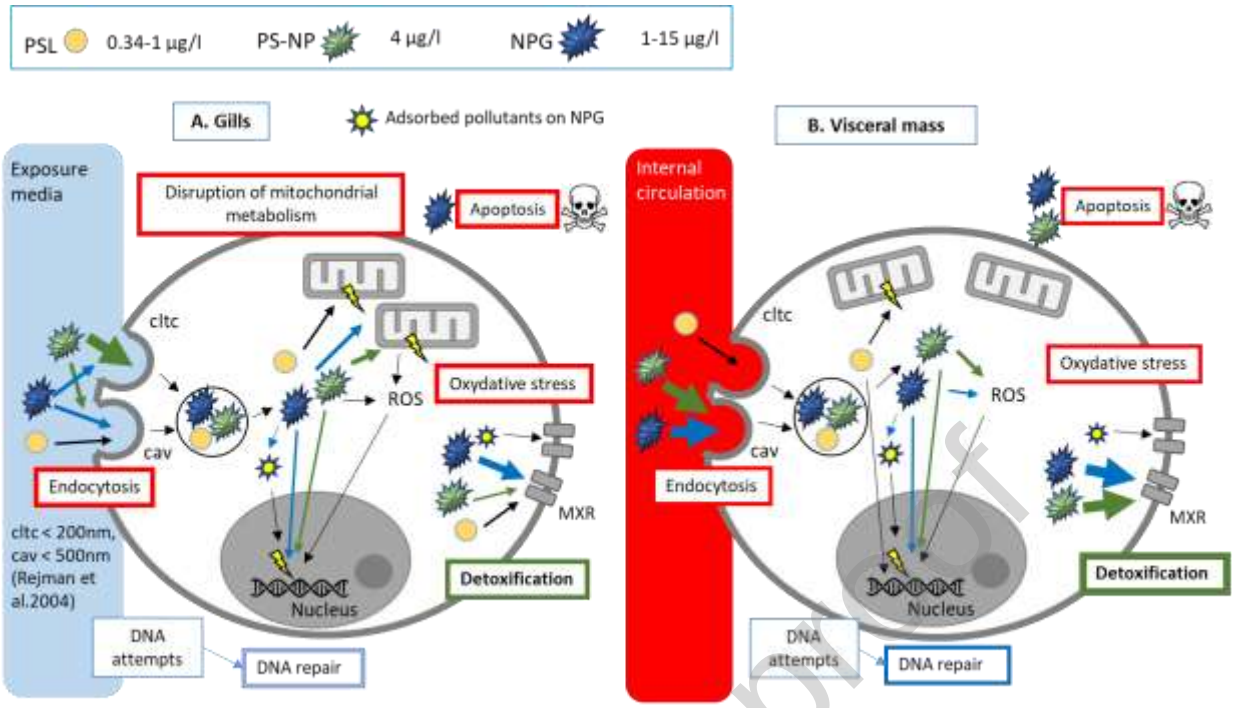

Figure 4 : Major routes of uptake, toxicity, and detoxification process for PSL, PS-NP, and NPG after exposure to low doses of oysters for 7 days in gills (A) and visceral mass (B). The thickness of arrows is related to the intensity of gene modulation.

CONCLUSION

We used microfluidic devices mimicking transition waters as observed in Guadeloupean swamps for the first time to disperse environmentally realistic NP solutions in a salinity gradient. Our results show the stabilization of NP of small sizes (< 500 nm) in the saline medium at the device's output. These NPs can be more easily taken up by cells of oysters *Isognomon alatus* via several endocytosis mechanisms compared to spiking experiments without simulated sanility gradients. Overall, results indicate that NP-G and NP-PS induced a higher response than PSL-COOH on expression of genes involved in processes such as endocytosis, mitochondrial metabolism disruption, oxidative stress, DNA repair, and detoxification, even at very low concentration (1-40 µg L^{-1}). At high concentrations, NP-G triggered more effects than NP-PS, as they are originated from the natural environment and could accumulate contaminants, enhancing toxicological effects. These findings underline the importance of the mode of exposure of organisms for ecotoxicological assessment, especially in transition waters, since salinity influences aggregation and the bioavailability and thus the effects of NPs.

Aknowledgements

We want to thank Pierre-Yves Pascal (UMR 7205, University of Antilles) for providing swamp oysters from Guadeloupe for the experiments. The French National Agency of Research funded this work (ANR-1-17-CE34-0008: PEPSEA). We thank Hind El Hadri from Cordouan Technologies for providing and analyzing the solutions of crushed nanoparticles.

Journal Pre-proof

Zélie Venel was a PhD student supported by a Cifre fund from ANRT and Cordouan Technologies.

References

Andrady, A.L., 2011. Microplastics in the marine environment. Mar. Pollut. Bull. 62, 1596–1605. https://doi.org/10.1016/j.marpolbul.2011.05.030

Anghelone, M., Jembrih-Simbürger, D., & Schreiner, M. 2014. Micro-Raman and ATR-FTIR for the study of modern paints containing synthetic organic pigments (SOPs): characterization of the photodegradation processes. In 11th Infrared and Raman Users Group Conference 5-7 November 2014 Museum of Fine Arts, Boston (p. 1).

Arini, A., Gigault, J, Venel, Z., Bertucci, A., Baudrimont, M., 2022. The underestimated toxic effects of NPs coming from marine sources: a demonstration on oysters (*Isognomon alatus*). Chemosphere, 295, 133824

Arini, A., Daffe, G., Gonzalez, P., Feurtet-Mazel, A., Baudrimont, M., 2014. What are the outcomes of industrial remediation on a metal-impacted hydrosystem? A 2-year field biomonitoring of the filter-feeding bivalve Corbicula fluminea. Chemosphere 108, 214–224. https://doi.org/10.1016/j. Chemosphere.2014.01.042

Barjhoux, I., Baudrimont, M., Morin, B., Landi, L., Gonzalez, P., Cachot, J., 2012. Effects of copper and cadmium spiked-sediments on embryonic development of Japanese medaka (Oryzias latipes). Ecotoxicol. Environ. Saf. 79, 272–282. https://doi.org/10.1016/j.ecoenv.2012.01.011

Baudrimont, M., Arini, A., Guégan, C., Venel, Z., Gigault, J., Pedrono, B., Prunier, J., Maurice, L., Ter Halle, A., Feurtet-Mazel, A., 2020. Ecotoxicity of polyethylene NPs from the North Atlantic oceanic gyre on freshwater and marine organisms (microalgae and filter-feeding bivalves). Environ. Sci. Pollut. Res. 27, 3746–3755. https://doi.org/10.1007/s11356-019-04668-3

Baudrimont, M., Schäfer, J., Marie, V., Maury-Brachet, R., Bossy, C., Boudou, A., Blanc, G., 2005. Geochemical survey and metal bioaccumulation of three bivalve species (Crassostrea gigas, Cerastoderma edule and Ruditapes philippinarum) in the Nord Médoc salt marshes (Gironde estuary, France). Sci. Total Environ. 337, 265–280. https://doi.org/https://doi.org/10.1016/j.scitotenv.2004.07.009

Catrouillet, C., Davranche, M., Khatib, I., Fauny, C., Wahl, A., & Gigault, J., 2021. Metals in microplastics: determining which are additive, adsorbed, and bioavailable. *Environmental Science: Processes & Impacts*, *23*, 553-558.

Chen, K.L., Elimelech, M., 2006. Aggregation and deposition kinetics of fullerene (C60) nanoparticles. Langmuir 22, 10994–11001. https://doi.org/10.1021/la062072v

Cole, M., Lindeque, P., Halsband, C., Galloway, T.S., 2011. Microplastics as contaminants in the marine environment: A review. Mar. Pollut. Bull. 62, 2588–2597. https://doi.org/10.1016/j.marpolbul.2011.09.025

El Hadri, H., Gigault, J., Maxit, B., Grassl, B., Reynaud, S., 2020. Nanoplastic from mechanically degraded primary and secondary microplastics for environmental assessments. NanoImpact 17, 100206. https://doi.org/10.1016/j.impact.2019.100206

Freitas, R., Coppola, F., De Marchi, L., Codella, V., Pretti, C., Chiellini, F., Morelli, A., Polese, G., Soares, A.M.V.M., Figueira, E., 2018. The influence of Arsenic on the toxicity of carbon nanoparticles in bivalves. J. Hazard. Mater. 358, 484–493. https://doi.org/10.1016/j.jhazmat.2018.05.056

Gigault, J., Halle, A. ter, Baudrimont, M., Pascal, P.Y., Gauffre, F., Phi, T.L., El Hadri, H., Grassl, B., Reynaud, S., 2018. Current opinion: What is a nanoplastic? Environ. Pollut. 235, 1030–1034. https://doi.org/10.1016/j.envpol.2018.01.024

Gigault, J., El Hadri, H., Nguyen, B. Grass, B., Rowenczyk, L., Tufenkji, N., Feng, S., Wiesner, M., 2021. Nanoplastics are neither microplastics nor engineered nanoparticles. Nat. Nanotechnol. 16, 501–507 .

Gonzalez, P., Baudrimont, M., Boudou, A., Bourdineaud, J.P., 2006. Comparative effects of direct cadmium contamination on gene expression in the zebrafish's gills, liver, skeletal muscles, and brain (Danio rerio). BioMetals 19, 225–235. https://doi.org/10.1007/s10534-005-5670-x

Haegerbaeumer, A., Mueller, M.T., Fueser, H., Traunspurger, W., 2019. Impacts of micro-and nano-sized plastic particles on benthic invertebrates: A literature review and gap analysis. Front. Environ. Sci. 7. https://doi.org/10.3389/fenvs.2019.00017

Handy, R.D., Henry, T.B., Scown, T.M., Johnston, B.D., Tyler, C.R., 2008. Manufactured nanoparticles: Their uptake and effects on fish - A mechanistic analysis. Ecotoxicology 17, 396–409. https://doi.org/10.1007/s10646-008-0205-1

Hrenovic, J., Ivankovic, T., 2007. Toxicity of anionic and cationic surfactant to Acinetobacter junii in pure

Journal Pre-proof

culture. Cent. Eur. J. Biol. 2, 405–414. https://doi.org/10.2478/s11535-007-0029-7

Ivar do Sul, J.A., Costa, M.F., Silva-Cavalcanti, J.S., Araújo, M.C.B., 2014. Plastic debris retention and exportation by a mangrove forest patch. Mar. Pollut. Bull. 78, 252–257. https://doi.org/10.1016/j.marpolbul.2013.11.011

Jahan, K., Balzer, S., Mosto, P., 2008. Toxicity of nonionic surfactants. WIT Trans. Ecol. Environ. 110, 281–290. https://doi.org/10.2495/ETOX080301

Jeong, C.B., Won, E.J., Kang, H.M., Lee, M.C., Hwang, D.S., Hwang, U.K., Zhou, B., Souissi, S., Lee, S.J., Lee, J.S., 2016. Microplastic Size-Dependent Toxicity, Oxidative Stress Induction, and p-JNK and p-p38 Activation in the Monogonont Rotifer (Brachionus koreanus). Environ. Sci. Technol. 50, 8849–8857. https://doi.org/10.1021/acs.est.6b01441

Koelmans, A.A., Besseling, E., Shim, W.J., 2015. NPs in the Aquatic Environment. Critical Review, in: Bergmann, M., Gutow, L., Klages, M. (Eds.), Marine Anthropogenic Litter. Springer International Publishing, pp. 1–447. https://doi.org/10.1007/978-3-319-16510-3

Kögel, T., Bjorøy, Ø., Toto, B., Bienfait, A.M., Sanden, M., 2020. Micro- and nanoplastic toxicity on aquatic life: Determining factors. Sci. Total Environ. 709, 136050. https://doi.org/10.1016/j.scitotenv.2019.136050

Lebordais, M., Z. Venel, J. Gigault, V. S. Langlois, and M. Baudrimont. 2021. Molecular Impacts of Dietary Exposure to NPs Combined or Not with Arsenic in the Caribbean Mangrove Oysters (Isognomon alatus). Nanomaterials **11**:1151.

Lemer, S., 2019. Assembled and translated transcriptomes. https://doi.org/doi:10.7910/DVN/TQDJ5Y

Lithner, D., Damberg, J., Dave, G., Larsson, Å., 2009. Leachates from plastic consumer products - Screening for toxicity with Daphnia magna. Chemosphere 74, 1195–1200. https://doi.org/10.1016/j.chemosphere.2008.11.022

Lithner, D., Larsson, A., Dave, G., 2011. Environmental and health hazard ranking and assessment of plastic polymers based on chemical composition. Sci. Total Environ. 409, 3309–3324. https://doi.org/10.1016/j.scitotenv.2011.04.038

Livak, K.J., Schmittgen, T.D., 2001. Analysis of relative gene expression data using real-time quantitative PCR and the 2-ΔΔCT method. Methods 25, 402–408. https://doi.org/10.1006/meth.2001.1262

Lu, K., Qiao, R., An, H., Zhang, Y., 2018. Influence of microplastics on the accumulation and chronic toxic effects of cadmium in zebrafish (Danio rerio). Chemosphere 202, 514–520. https://doi.org/10.1016/j.chemosphere.2018.03.145

Manfra, L., Rotini, A., Bergami, E., Grassi, G., Faleri, C., Corsi, I., 2017. Comparative ecotoxicity of polystyrene nanoparticles in natural seawater and reconstituted seawater using the rotifer Brachionus plicatilis. Ecotoxicol. Environ. Saf. 145, 557–563. https://doi.org/10.1016/j.ecoenv.2017.07.068

Marigomez, I., Soto, M., Cajaraville, M.P., Angulo, E., Giamberini, L., 2002. Cellular and subcellular distribution of metals in molluscs. Microsc. Res. Tech. 56, 358–392. https://doi.org/10.1002/jemt.10040

Martin, C., Almahasheer, H., Duarte, C.M., 2019. Mangrove forests as traps for marine litter. Environ. Pollut. 247, 499–508. https://doi.org/10.1016/j.envpol.2019.01.067

Mo, Y. and Lim, L., 2004. Mechanistic study of the uptake of wheat germ agglutinin-conjugated PLGA nanoparticles by A549 cells. *Journal of pharmaceutical sciences*, *93*, 20-28.

Moreira, A., Figueira, E., Mestre, N.C., Schrama, D., Soares, A.M.V.M., Freitas, R., Bebianno, M.J., 2018. Impacts of the combined exposure to seawater acidification and arsenic on the proteome of Crassostrea angulata and Crassostrea gigas. Aquat. Toxicol. 203, 117–129. https://doi.org/10.1016/j.aquatox.2018.07.021

Pikuda, O., Xu, E.G., Berk, D., Tufenkji, N., 2019. Toxicity Assessments of Micro- and NPs Can Be Confounded by Preservatives in Commercial Formulations. Environ. Sci. Technol. Lett. 6, 21–25. https://doi.org/10.1021/acs.estlett.8b00614

Rejman, J., Oberle, V., Zuhorn, I.S., Hoekstra, D., 2004. Size-dependent internalization of particles via the pathways of clathrin-and caveolae-mediated endocytosis. Biochem. J. 377, 159–169. https://doi.org/10.1042/BJ20031253

Rochman, C.M., Manzano, C., Hentschel, B.T., Simonich, S.L.M., Hoh, E., 2013b. Polystyrene plastic: A source and sink for polycyclic aromatic hydrocarbons in the marine environment. Environ. Sci. Technol. 47, 13976–13984. https://doi.org/10.1021/es403605f

Rosety, M., Ordóñez, F.J., Rosety-Rodríguez, M., Rosety, J.M., Rosety, I., Carrasco, C., Ribelles, A., 2001. Acute toxicity of anionic surfactants sodium dodecyl sulphate (SDS) and linear alkylbenzene sulphonate (LAS) on the fertilizing capability of gilthead (Sparus aurata L.) sperm. Histol. Histopathol. 16, 839–843.

Journal Pre-proof

https://doi.org/10.14670/HH-16.839

Sajiki, J., Yonekubo, J., 2003. Leaching of bisphenol A (BPA) to seawater from polycarbonate plastic and its degradation by reactive oxygen species. Chemosphere 51, 55–62. https://doi.org/10.1016/S0045-6535(02)00789-0

Ter Halle, A., Jeanneau, L., Martignac, M., Jardé, E., Pedrono, B., Brach, L., Gigault, J., 2017. Nanoplastic in the North Atlantic Subtropical Gyre. Environ. Sci. Technol. 51, 13689–13697. https://doi.org/10.1021/acs.est.7b03667

Teuten, E.L., Saquing, J.M., Knappe, D.R.U., Barlaz, M.A., Jonsson, S., Björn, A., Rowland, S.J., Thompson, R.C., Galloway, T.S., Yamashita, R., Ochi, D., Watanuki, Y., Moore, C., Viet, P.H., Tana, T.S., Prudente, M., Boonyatumanond, R., Zakaria, M.P., Akkhavong, K., Ogata, Y., Hirai, H., Iwasa, S., Mizukawa, K., Hagino, Y., Imamura, A., Saha, M., Takada, H., 2009. Transport and release of chemicals from plastics to the environment and wildlife. Philos. Trans. R. Soc. B Biol. Sci. 364, 2027–2045. https://doi.org/10.1098/rstb.2008.0284

Velzeboer, I., Kwadijk, C.J.A.F., Koelmans, A.A., 2014. Strong sorption of PCBs to NPs, microplastics, carbon nanotubes, and fullerenes. Environ. Sci. Technol. 48, 4869–4876. https://doi.org/10.1021/es405721v

Venel, Z., Tabuteau, H., Pradel, A., Pascal, P. Y., Grassl, B., El Hadri, H., Baudrimont, M., Gigault, J., 2021. Environmental Fate Modeling of Nanoplastics in a Salinity Gradient Using a Lab-on-a-Chip: Where Does the Nanoscale Fraction of Plastic Debris Accumulate?. Environmental Science & Technology, 55: 3001-3008.

Wegner, A., E. Besseling, E. M. Foekema, P. Kamermans, and A. A. Koelmans. 2012. Effects of nanopolystyrene on the feeding behavior of the blue mussel (Mytilus edulis L.). Environmental Toxicology and Chemistry **31**:2490-2497.

Woods, M. N., M. E. Stack, D. M. Fields, S. D. Shaw, and P. A. Matrai. 2018. Microplastic fiber uptake, ingestion, and egestion rates in the blue mussel (Mytilus edulis). Mar Pollut Bull **137**:638-645.

Yin, J., Deng, X., Zhang, J., Lin, J., 2018. Current Understanding of Interactions between Nanoparticles and ABC Transporters in Cancer Cells. Curr. Med. Chem. 25, 5930–5944. https://doi.org/10.2174/0929867325666180314122200

CRediT authorship contribution statement

Adeline Arini : Investigation, methodology, formal analysis,validation, writing – original draft. Zélie Venel : Investigation, methodology, formal analysis, writing – original draft. Hervé Tabuteau : Methodology, writing – review & editing. Julien Gigault : Conceptualization, methodology, funding acquisition, resources, supervision, writing – review & editing. Magalie Baudrimont : Conceptualization, methodology, funding acquisition, resources, supervision, validation, writing – review & editing

Declaration of Competing Interest

☒ The authors declare that they have no known competing financial interests or personal relationships that could have appeared to influence the work reported in this paper.

☐ The authors declare the following financial interests/personal relationships which may be considered as potential competing interests:

Graphical abstract

Journal Pre-proof

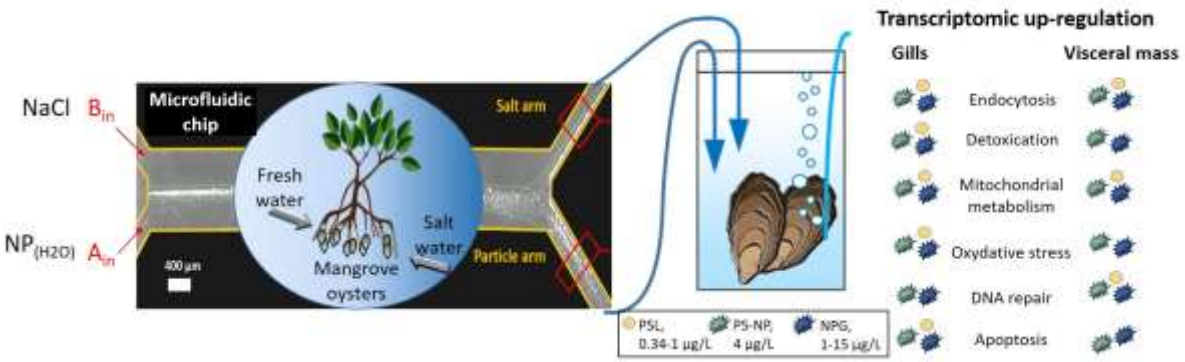

Highlights

- . First use of a microfluidic device to mimick a salinity gradient and expose oysters
- . Low aggregation of NPs in the salinity gradient using a microfluidic device
- . Up-regulation of genes (*12s*, *sod1*, *cat*, *bax*) at low NPs concentrations, from 1µg/L
- . More adverse effects after exposure to environmental NPs versus polystyrene ones.

Journal Pre-proof